NMR Spectroscopy in the Presence of Strong Ac Electric Fields: Degree of Alignment of Polar Molecules

Alexey Peshkovsky and Ann E. McDermott*

Department of Chemistry, Columbia University, New York, New York 10027

Received: June 17, 1999; In Final Form: August 18, 1999

We report NMR spectra of nitrobenzene-d_5 recorded in the presence of strong ac electric fields using a home-built probe and electric field amplifier. Pulsed ac electric fields up to 70 kV/cm rms were used, rather than dc fields, to reduce electrode corrosion, electrode polarization, electrical convection, sensitivity to impurities, electrolysis, and heating. A two-dimensional detection method was used in which fields are applied only during the variable delay associated with the indirect dimension. Tensorial interactions are partially recovered due to partial alignment of the polar molecules in the applied electric field. Molecular order parameters of order 10^{-4} were observed in these experiments, in agreement with previous work, and followed the expression $S_{mol} \propto E^2$, as expected, where the constant of proportionality describes the effects of the dielectric response of the medium. Deuterium splittings for the ortho- and paradeuterons were in the ratios expected for a 61° relative angle in bond vectors. We observed a strong dependence of the order parameter on concentration: neat nitrobenzene ordered significantly more than did nitrobenzene diluted in a nonpolar solvent. Under the assumption that neat nitrobenzene forms weakly bound clusters with large effective dipole moments, we attempted to rationalize the degree of order for dilute nitrobenzene only in terms of simple electrostatic theories. Onsager's model involving spherical molecules overestimates the alignment while Scholte's adaptation of Onsager's model for elliptical molecules achieves reasonable agreement with our data for dilute nitrobenzene.

Introduction

Polarization of materials in the presence of electric fields has been a subject of research for a long time. Because NMR can provide descriptions of molecular conformation, orientation, and dynamics, the response of molecules to electric fields can be studied in detail when an electric field is applied during NMR observation. Interest in NMR of partially aligned solutions has had a resurgence recently, motivated by the opportunity to measure dipolar splittings in liquids.[1−4] Changes in molecular orientation ("orientation polarization") can be studied in liquids, while electronic and nuclear rearrangements within the molecule ("electronic polarization" and "atomic polarization") can be studied in solids. "Distortion polarization" (a combination of electronic and atomic polarization) has been detected by Kushida and Saiki,[5] as well as Armstrong, Bloembergen, and Gill[6] who observed a change in the quadrupolar coupling constants of nuclei in crystals only at the sites which lack inversion symmetry in the presence of an external dc electric field. Gill and Bloembergen,[7] as well as Collins and Bloembergen,[8] showed that these effects are due to both the electronic polarization and the ionic displacements which cause the local electric field gradients to change.

Numerous studies have shown that large dc fields polarize molecules in liquids. Liquids can become doubly refracting when placed in strong electric fields due to orientation polarization (Kerr effect). This effect, discovered by John Kerr in 1875, is routinely used to make optical shutters or gates. NMR studies of the effects of the externally applied dc electric fields on orientation of molecules with high dipole moments in insulating liquids, such as nitrobenzene or acetonitrile, have been reviewed by Hilbers and MacLean,[9] including theoretical background and a description of measurements of quadrupolar (for ^{14}N) and dipolar (for ^{1}H) splittings arising from the residual molecular ordering. Huis, Decanter, and MacLean[10] determined the shielding anisotropy for ^{13}C in acetonitrile using a similar experimental setup. Plantega, Van Zijl, and MacLean[11] described the measurements of the quadrupolar splitting for ^{2}H in pure nitrobenzene-d_5, as well as in perdeuterated nitrobenzene/ethylenecarbonate, nitrobenzene/acetonitrile, and acetonitrile/benzene mixtures, arising from the dielectric orientation by a dc electric field. Biemond and MacLean[12] performed experiments involving dc electric fields applied to mixtures of nitrobenzene-d_5 with nonpolar solvents.

In this paper, we report a series of experiments in which we observed the deuteron quadrupolar splitting due to the partial alignment of nitrobenzene-d_5 under the influence of ac electric field, as a function of the field strength (up to 70 kV/cm (rms)), as well as a function of concentration in nonpolar solvent and of temperature. Pulsed ac electric fields were utilized to reduce complications due to sample impurities, which were encountered in the previous studies. The use of kilohertz ac electric fields reduces many deleterious processes, such as electrolytic sample and electrode degradation, electrical convection, and electrode polarization. Exposing samples to pulsed rather than constant fields further reduces these effects, and alleviates ohmic heating. In our experiments no additional purification of commercial nitrobenzene-d_5 (99.5% atom D) was required. Furthermore, 2D methods were used, such that the electric fields were not present during the NMR signal detection. The conductivity of pure nitrobenzene and its solutions in nonpolar solvents is very low. Therefore, these samples are significantly more forgiving in terms of the technical difficulties mentioned above than, for example, the aqueous solutions of biological molecules, where some of the effects can become prohibitive. Further interesting application of these methods will require solving several technical problems.

10.1021/jp991993u CCC: $18.00
Published on Web 10/14/1999

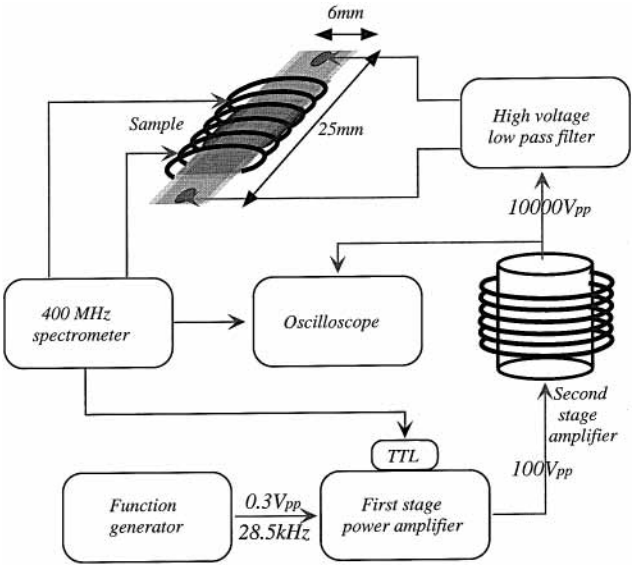

Figure 1. Schematic describing the experimental apparatus. The output of a function generator is amplified in two stages. The first stage is a 200 W home-built power amplifier, which is capable of producing a 100 V_{pp} signal. This stage is equipped with a TTL trigger input, which allows for synchronization with an NMR pulse train. The second stage is a home-built passive voltage amplifier, which consists of an inductor L in series with a capacitor C. On resonance, this device performs 100-fold voltage amplification (see text for more details). A home-built three-stage high-voltage low-pass filter removes the rf noise from the high-voltage line, greatly reducing the spectral contamination. The high-voltage pulses are monitored with an oscilloscope.

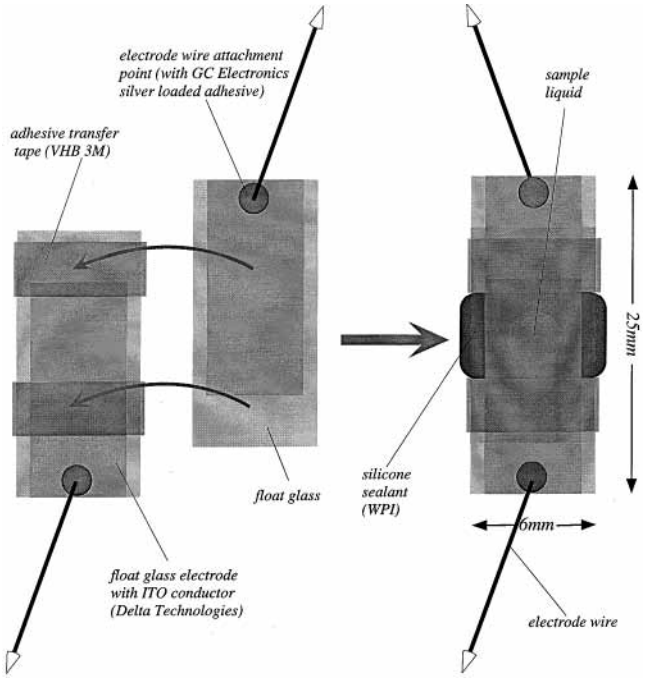

Figure 2. Sample cell "sandwich". Adhesive transfer tape serves as a calibrated spacer between ITO electrodes. After the electrodes are attached together, silicone sealant is deposited between them, leaving a bubble in the middle for the sample. Liquid samples are injected through the sealant into the bubble, while the air is relieved. Samples so made were 400 μm thick liquid disks, approximately 2 mm in diameter.

Experimental Section

We utilized a home-built two-stage high-voltage generator capable of delivering up to 10 kV_{pp} (V_{pp} = peak to peak volts) ac with frequencies from 20 to 40 kHz. The modulation frequency for the electric field varied by a few tens of hertz around 28.5 kHz, depending on the sample cell's capacitance. Liquid samples were injected into a 400 μm gap between indium tin oxide (ITO) glass electrodes. The experiments were conducted on a CMX-400 wide bore Chemagnetics solid state spectrometer. Nitrobenzene-d_5 was obtained from Aldrich (Milwaukee, WI). The applied voltage was monitored with the TDS 210 Tektronix (Wilsonville, OR) oscilloscope. The estimated error in measuring the applied electric field, including both the voltage and the interelectrode distance measurements, was less than 5%. The experimental setup is illustrated in Figure 1. A detailed description of the equipment and the techniques used in this experiment follows.

High-Voltage Generator. The high voltage generator consisted of two stages. The first stage was a home-built linear power amplifier driven by the DS345 Stanford Research Systems (Sunnyvale, CA) function generator. It was capable of delivering 200 W at 100 Vpp and had a TTL trigger input allowing the high-voltage pulses to be synchronized with the spectrometer pulse sequence. The second stage was a passive voltage amplifier, which consisted of an inductor, L, in series with a capacitor, C. The inductor was wound in a single layer around a cylindrical spool of 250 mm o.d. and 350 mm in length with a 25-gauge wire. The coaxial cable that went from the second stage to a sample in the probe served also as the capacitor C in series with the inductor L and in parallel to a sample cell. The impedance for such device can be expressed as

$$Z = i\left[L\omega - \frac{1}{C\omega}\right] + R \qquad (1)$$

where R represents the active losses in the circuit. On resonance when the frequency $\omega = 1/\sqrt{LC}$, $Z = R$, and current $I(t)$ that flows through every element in this circuit, including C, is

$$I(t) = \frac{V_{in}(t)}{R} = iV_c(t)C\omega \qquad (2)$$

where $V_{in}(t)$ is the voltage applied to the circuit and $V_c(t)$ is the voltage across the capacitor. Making the substitution gives

$$V_c(t) = -iV_{in}(t)\frac{\sqrt{L}}{R\sqrt{C}} = -iQuV_{in}(t) \qquad (3)$$

where Qu is the quality factor for this circuit, which was experimentally found to be 100. This 100-fold amplified and 90° phase-shifted voltage across the capacitor C was delivered to the sample.

Sample Cells. Sample cells were made from indium tin oxide (ITO) coated glass electrodes (6 mm by 25 mm), purchased from Delta Technologies (Stillwater, MN), which were etched to remove the conductor from 1 mm along the edges to prevent breakdown through air around the edges. The electrodes were spaced by 400 μm using the 3M Scotch VHB (St. Paul, MN) adhesive transfer tape. The remaining space between the electrodes was filled with the 2 part 5 minute silicone sealant (purchased from World Precision Instruments, Sarasota, FL) with a round flat bubble left in the middle. Electrode wires were attached to the conducting surfaces using silver-loaded adhesive (purchased from GC Electronics, Greensboro, NC) and attachment spots were covered with epoxy. Samples were injected with a syringe through the elastic silicone sealant using two 33-gauge needles, one to deliver the liquid and the other to relieve the air. Figure 2 illustrates the glass electrodes and the cell "sandwich" in detail. This design is quite different from

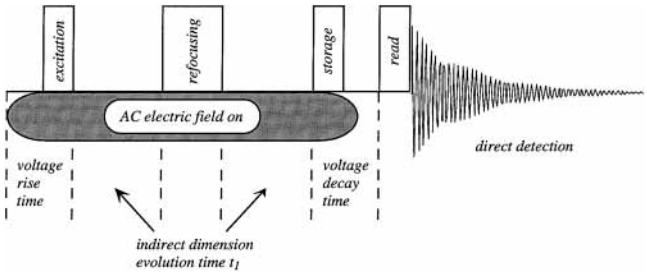

Figure 3. Pulse sequence used for the detection of the electric field effect. The ac electric field is on during the evolution time t_1 and off during the acquisition and the recycle delay. A single refocusing pulse removes the chemical shift offset and the $\mathbf{B}_0$ inhomogeneity effects. The resulting 2D spectra have the isotropic chemical shifts in the direct dimension and the electric field induced splitting in the indirect dimension.

the one used in the earlier studies of the degree of molecular alignment[9] and is similar to the arrangement used by Peter Osman and Bruce Cornell.[13] Because the area of the electrodes is significantly larger than the distance between them and no part of the sample is near the edges, high degree of electric field homogeneity is achieved, thus minimizing electrophoretic convection and indirect dimension broadening.

Pulse Sequence. The pulse sequence is shown in Figure 3. Two-dimensional data acquisition was used so that the direct dimension of our spectra was the isotropic chemical shift and the indirect dimension was the electric field induced splitting. Five milliseconds before the rf excitation pulse, a TTL (transistor−transistor logic) "high" was given by the spectrometer to the first amplification stage of the high-voltage generator initiating a high-voltage pulse. After the rf storage pulse the TTL level was switched to "low". Thus, the high-voltage pulse was off during the acquisition and its length was incremented together with the indirect dimension time t_1. The rf pulse in the middle of the t_1 interval refocused the chemical shift and the dephasing due to $\mathbf{H_0}$ inhomogeneity, but did not refocus the evolution under the quadrupolar Hamiltonian. Line widths in this dimension reflect the electric field inhomogeneity and T_2 relaxation.

Theory

For a spin $\mathbf{I} = 1$ nucleus in a dipolar molecule in a high magnetic field approximation the Hamiltonian can be expressed as[9,14]

$$H = -\hbar\gamma \mathrm{H}_0 I_{z'} + \frac{eQ}{4I(I+1)} V_{z'z'}(3I_{z'}{}^2 - I^2) \qquad (4)$$

where Q is the quadrupole moment of the nucleus, γ is the gyromagnetic ratio of the nucleus, the magnetic field $\mathbf{H_0}$ is in the $\mathbf{z'}$ direction in the laboratory coordinate frame (LAB), $I_{z'}$ is the component of $\mathbf{I}$ along $\mathbf{z'}$ and $V_{z'z'}$ is the tensor element describing the electric field gradient at the nucleus in the LAB. In the case of nitrobenzene-d_5, where the C−D bond is assumed to possess approximate cylindrical symmetry, $\mathbf{V}_{z'z'}$ in the LAB can be related to $\mathbf{V}_{zz} = \sqrt{3/2}eq$ in the principal axes coordinate frame (PAS) by the expression:[15]

$$V_{z'z'} = V_{zz} \sum_{q=-2}^{2} D_{0q}^{(2)}(\alpha_1,\theta_1,\gamma_1) D_{q0}^{(2)}(\alpha,\theta,\gamma) \qquad (5)$$

In this expression $D_{0q}^{(2)}$ and $D_{q0}^{(2)}$ are the Wigner rotation matrices, eq is the quadrupolar coupling parameter, α_1, θ_1, and γ_1 are the Euler angles between the PAS and the molecular fixed coordinate frame adopted to the direction of the molecular dipole moment $\mathbf{p}$ (MFF) and α, θ and γ are the Euler angles between the MFF and the LAB.

The energy levels are obtained if this expression is expanded and substituted into (4). The frequencies in Hz of the single quantum transitions between these levels differ by

$$\Delta\nu = \pm\frac{3}{2}\frac{e^2qQ}{h}\left[\left(\frac{3}{2}\cos^2\theta - \frac{1}{2}\right)\left(\frac{3}{2}\cos^2\theta_1 - \frac{1}{2}\right) - \frac{3}{4}\sin 2\theta_1 \sin 2\theta \cos(\alpha_1 + \gamma) + \frac{3}{4}\sin^2\theta_1 \sin^2\theta \cos 2(\alpha_1 + \gamma)\right] \qquad (6)$$

The molecular tumbling causes $\Delta\nu$ to be averaged over all values of the angles θ and γ, and every term of this expression disappears. When an electric field $\mathbf{E}$ is applied, partial ordering of the molecules occurs on the basis of their dipole moments. The term containing θ no longer averages to zero, while both terms containing γ still do. If $\mathbf{E}$ is parallel to $\mathbf{H_0}$ then the expected quadrupolar splitting in Hz can be expressed as

$$\Delta\nu = \frac{3}{2}\frac{e^2qQ}{h}\left\langle\frac{3}{2}\cos^2\theta - \frac{1}{2}\right\rangle_E\left(\frac{3}{2}\cos^2\theta_1 - \frac{1}{2}\right) \qquad (7)$$

where the angled brackets $\langle\ \rangle$ denote an ensemble/time average. The molecular order parameter $S_{\mathrm{mol}} = \langle({}^3/_2\cos^2\theta - {}^1/_2)\rangle_{\mathrm{E}}$ describes the molecular alignment averaged over the Brownian motion. The factor $({}^3/_2\cos^2\theta_1 - {}^1/_2)$ differs for the para- and ortho- or metadeuterons because their C−D bond vectors are at 0°, 60°, and 120° angles (θ_1) with respect to the molecular dipole moment $\mathbf{p}$.[16] We assumed a deuterium quadrupolar coupling constant e^2qQ/h for nitrobenzene of 192 kHz.[17,18]

The potential energy $\mathbf{U}$ of a dipole $\mathbf{p}$ at an angle θ to an electric field $\mathbf{E}$ is

$$U = -pE\cos\theta \qquad (8)$$

According to Boltzmann's law, the probability P of the dipole being at an angle θ to the direction of the field is[19]

$$P = \frac{\mathrm{e}^{-pE\cos\theta/kT}\,\mathrm{d}\omega}{\int \mathrm{e}^{-pE\cos\theta/kT}\,\mathrm{d}\omega} \qquad (9)$$

where k is the Boltzmann's constant, T is the temperature, and $\mathrm{d}\omega = 2\pi\sin\theta\,\mathrm{d}\theta$.

If an electric field $\mathbf{E}$ is applied to a dipolar liquid, Boltzmann's law gives the following time-weighted average (second Legendre) function of the molecular polar angle, or molecular order parameter:[9]

$$S_{\mathrm{mol}} = \left\langle\frac{3}{2}\cos^2\theta - \frac{1}{2}\right\rangle = \frac{\int({}^3/_2\cos^2\theta - {}^1/_2)\mathrm{e}^{-p_{\mathrm{eff}}E_d\cos\theta/kT}\,\mathrm{d}\cos\theta}{\int \mathrm{e}^{-p_{\mathrm{eff}}E_d\cos\theta/kT}\,\mathrm{d}\cos\theta} \qquad (10)$$

In this expression $\mathbf{E}_{\mathrm{d}}$ is the *directing* field responsible for the ordering of the molecules, which is different from the *applied* field $\mathbf{E}$ due to the screening of the field by the surroundings of the dipole and $\mathbf{p}_{\mathrm{eff}}$ is the effective dipole moment of the polarizable molecules in the liquid. The effective dipole moment is larger than the corresponding dipole moment $\mathbf{p}$ for the same

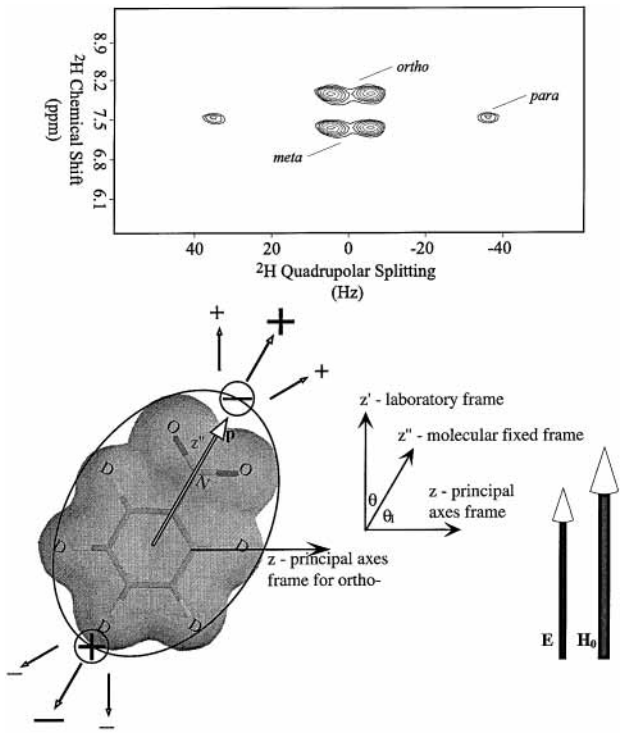

Figure 4. Geometry of the experiment and a 2D spectrum of pure nitrobenzene-d_5 at 70 kV/cm (rms) at 298 K. The direct (vertical) dimension contains the isotropic shift information for meta-, para-, and orthodeuterons (in the order of increasing resonance frequency). The indirect (horizontal) dimension contains the electric field induced quadrupolar splittings. Magnetic $\mathbf{H}_0$ and electric $\mathbf{E}$ fields are parallel to each other. Molecular fixed frame $\mathbf{z}''$-axis of nitrobenzene-d_5 is at an angle θ to the laboratory frame $\mathbf{z}'$-axis. Principal axes frame $\mathbf{z}$-axes along C−D bonds with para-, meta-, and orthodeuterons are at $\theta_1 = 0°$, 120°, and 60° to the molecular fixed frame $\mathbf{z}''$-axis. The polarizing effect of the "reaction" field is indicated by small arrows "stretching" the molecule. This reaction field is created due to the rapid polarization of the environment of the molecule by its permanent dipole.

molecules in a gas phase due to the additional polarization by the *reaction* field $\mathbf{E}_r$. When a dipole polarizes its surrounding medium, a reaction field is created at the dipole's location in response. Thus, the total field acting on the dipole can be considered as a sum of the *cavity* field $\mathbf{E}_c$, or the field that would exist in a cavity formed by removing the central molecule, and the reaction field $\mathbf{E}_r$. As is shown in Figure 4, $\mathbf{E}_r$ polarizes the dipole, changing its dipole moment from $\mathbf{p}$ to $\mathbf{p}_{eff}$, but, because it is parallel to the dipole vector, it does not participate in the ordering. The directing field $\mathbf{E}_d$, therefore, equals the cavity field $\mathbf{E}_c$. As a result of these effects, the energy is offset from the product $\mathbf{pE}$ by a fixed scaling factor. In order to model the extent of alignment quantitatively, a shape for the molecule and a dielectric constant for the medium were assumed, as discussed in the following.

Onsager's Model. This model assumes that molecules in solution occupy spherical cavities.[20] The effect of the reaction field is included in the expression for $\mathbf{p}_{eff}$:[21]

$$p_{eff} = \frac{2\epsilon + 1}{2\epsilon + {n_D}^2} \frac{{n_D}^2 + 2}{3} p \tag{11}$$

where ϵ is the static dielectric constant of the medium and n_D is the refractive index of the molecule in question. ${n_D}^2$ is approximately equal to the dielectric constant, if the frequency is high enough for the orientation polarization to become unimportant (typically GHz for small molecules in liquids), while both the atomic and the electronic polarizations remain active.[21] For pure nitrobenzene[21] $\epsilon = 35$, ${n_D}^2 = 2.4$, $\mathbf{p} = 4.2$ D, and $\mathbf{p}_{eff} = 6.0$ D. The value for the dipole is based on gas phase measurements and is in reasonable agreement with ab initio calculations (<10% discrepancy among experimental values or between experiment and calculation). The directing field is taken as

$$E_d = E_c = \frac{3\epsilon}{2\epsilon + 1} E \tag{12}$$

Scholte's Model. Scholte adapted Onsager's theory to nonspherical molecules[22] by deriving the expression for the reaction field in an ellipsoidal cavity. A near-elliptical shape of the molecule of nitrobenzene was obtained from the ab initio HF (STO-3G) calculations of the electronic density surface in Spartan. The Spartan default value of 0.002 electrons/au^3 for the evaluation of molecular size and shape was chosen for the surface boundary. When an external electric field is applied in the direction of the *a*-axis of the ellipsoid with the principal axes 2*a*, 2*b*, and 2*c* the cavity field can be given by the following expression:[21]

$$E_c = E_d = \frac{\epsilon}{\epsilon + (1 - \epsilon)A_a} E \tag{13}$$

The factor A_a depends on the shape of the ellipsoid and is given by

$$A_a = \frac{abc}{2} \int_0^\infty \frac{ds}{(s + \alpha^2)R} \tag{14}$$

where $\alpha = a$, b, c, and $R = [(s + a^2)(s + b^2)(s + c^2)]^{1/2}$. The energy of the dipole in an electric field is proportional to the component of the cavity field in the *a*-direction, given by (13).[9] When the effects of the reaction field are taken into consideration the expression for $\mathbf{p}_{eff}$ can be written as follows:[21]

$$p_{eff} = \frac{\{\epsilon + (1 - \epsilon)A_a\}\{1 + ({n_D}^2 - 1)A_a\}}{\epsilon + ({n_D}^2 - \epsilon)A_a} p \tag{15}$$

where ${n_D}^2$ is used as a dielectric constant of the molecule in the cavity.

Calculations of the Splitting Values. If the exponential in (10) is expanded in a power series and if electric saturation is ignored,[21] a simple relationship between the order parameter, the directing field, and the effective dipole moment can be obtained which is valid in the high-temperature limit, $pE/kT \ll 1$:[9]

$$S_{mol} = \left\langle \frac{3}{2} \cos^2 \theta - \frac{1}{2} \right\rangle_E = \frac{1}{15} \left[\frac{p_{eff} E_d}{kT} \right]^2 \tag{16}$$

Under the influence of a rapidly oscillating field, the quadrupolar splitting is proportional to the time average of $\mathbf{E}^2 \cos^2(\omega_{mod} t$, or $\mathbf{E}_{rms}{}^2$ in the limit that the oscillation frequency of the electric field ω_{mod} is much greater than splitting. Onsager's model leads to the following expression for the splitting in Hz for para-deuteron:

$$\Delta\nu_{Ons} = \frac{1}{10} \frac{e^2 qQ}{h} \left[\frac{p}{kT} \frac{\epsilon({n_D}^2 + 2)}{2\epsilon + {n_D}^2} \right]^2 {E_{rms}}^2 \tag{17}$$

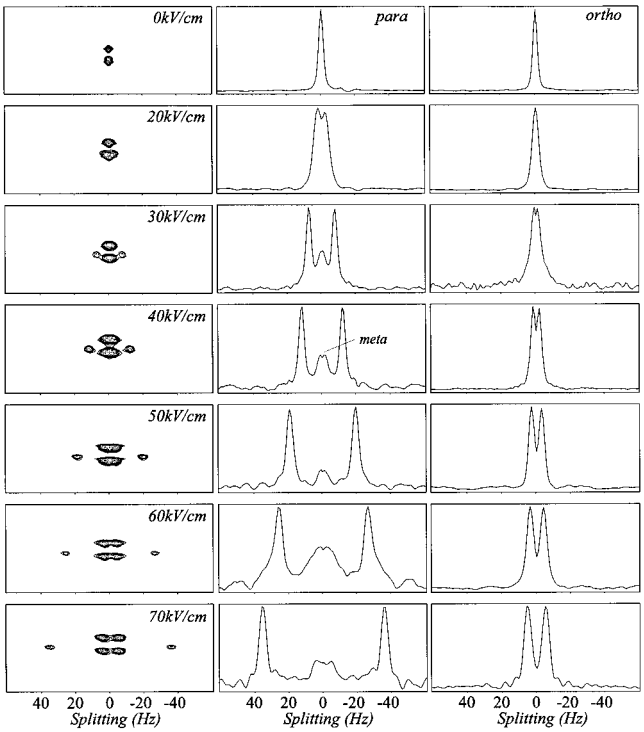

Figure 5. Deuterium spectra of nitrobenzene-d_5 in the presence of ac electric fields at 298 K. The rms values of the applied fields are indicated on the two-dimensional plots in the left column. The indirect dimension slices for para- and orthodeuterons are shown in the middle and the right columns. The ratios of the splittings are as expected for a 61° relative angle in bond vectors.

Scholte's model gives:

$$\Delta\nu_{\mathrm{Sch}} = \frac{1}{10}\frac{e^2qQ}{h}\left[\frac{p}{kT}\frac{\epsilon\{1+(n_{\mathrm{D}}{}^2-1)A_{\mathrm{a}}\}}{\epsilon+(n_{\mathrm{D}}{}^2-\epsilon)A_{\mathrm{a}}}\right]^2 E_{\mathrm{rms}}{}^2 \quad (18)$$

The results of an ab initio HF (STO-3G) calculations of the electronic density surface of nitrobenzene (Spartan) lead to the ratios $c/a = 0.35$ and $b/a = 0.68$ for the elliptical axes, which correspond to $A_{\mathrm{a}} = 0.16$.[23] Substituting these values for the constants gives (in Hz):

$$\Delta\nu_{\mathrm{Ons}} = \frac{3}{2}\frac{e^2qQ}{h}\,3.51\times10^{-18}E_{\mathrm{rms}}{}^2 = 1.01\times10^{-12}E_{\mathrm{rms}}{}^2 \quad (19)$$

and

$$\Delta\nu_{\mathrm{Sch}} = \frac{3}{2}\frac{e^2qQ}{h}\,1.60\times10^{-18}E_{\mathrm{rms}}{}^2 = 0.46\times10^{-12}E_{\mathrm{rms}}{}^2 \quad (20)$$

It is important to point out that because in Scholte's model the ratio and not the size of the elliptical dimensions is important, the calculated splitting values are not very sensitive to the density surface boundary parameters used in the quantum chemical calculations. For instance, if the density surface boundary is set to half of its default value, A_{a} becomes 0.18[23] and the changes in the calculated splitting are less than 10%.

Results and Discussion

The experimental geometry is illustrated in Figure 4.

Field Strength Dependence. The 2D and the indirect dimension spectra for para- and orthodeuterons of pure nitrobenzene-d_5 in the presence of various ac electric fields are shown in Figure 5. The electric field induced splitting values for para-, ortho-, and metadeuterons, as well as the values predicted by Onsager's and Scholte's models for paradeuterons are indicated in Table 1 and plotted as a function of the square of the applied field in Figure 6. The experimental relationship between the splitting in Hz and the square of the electric field for paradeuterons, based on a linear fit is

$$\Delta\nu = \frac{3}{2}\frac{e^2qQ}{h}\,5.24\times10^{-18}E^2 = 1.51\times10^{-12}E^2 \quad (21)$$

The data depend on $\mathbf{E^2}$ as expected, suggesting that heating artifacts are minimal. The ratio of the splitting values for para- and orthodeuterons is 6.7 ± 0.3 and is consistent with a polar

TABLE 1: Experimental and Theoretical Splitting Values (in Hz) for Nitrobenzene-d_5 at Various Electric Fields[a,b]

$E_{\mathrm{rms}}{}^2 \times 10^8$ (V^2/cm^2)	para-	ortho-, meta-	Onsager's model for para-	Scholte's model for para-
0.0	0.0	0.0	0.0	0.0
4.0	5.3	0.9	4.0	1.8
9.0	15.6	2.0	9.0	4.1
16.0	24.2	3.9	16.1	7.3
25.0	39.0	6.0	25.1	11.5
36.0	52.6	8.1	36.1	16.5
49.0	71.5	10.7	49.2	22.5

[a] Taken at 298 K in the presence of electric fields up to 70 kV/cm (rms). [b] The measurement error in the splitting values was estimated to be 0.5 Hz.

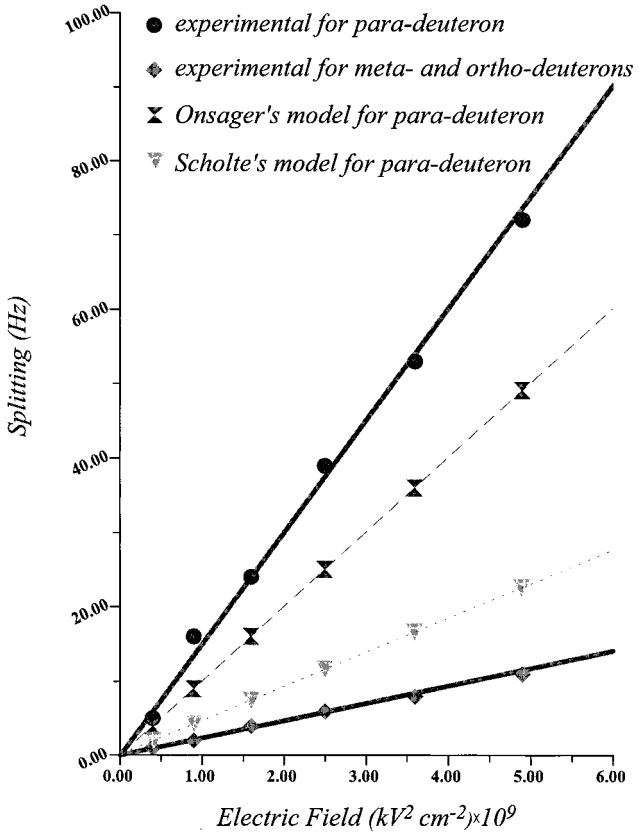

Figure 6. Dependence of the experimental para-, ortho-, and meta-deuteron's quadrupolar splitting values and the values calculated using Onsager's and Scholte's models for paradeuteron on the square of the external ac electric field due to partial dipole alignment. The horizontal axis shows the rms squared values of the field. The experimental values closely follow the square of the field, although the slope differs from that predicted theoretically. We assume that this discrepancy is due to intermolecular interactions that result in large effective dipole moments.

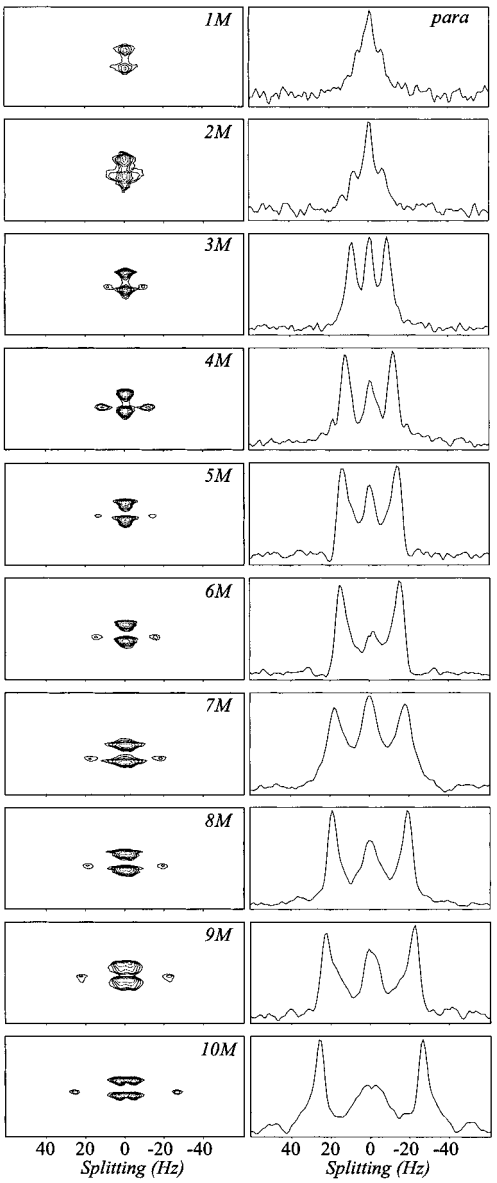

Figure 7. Deuterium spectra of nitrobenzene-d_5 at different concentrations in nonpolar solvents in the presence of a 60 kV/cm (rms) external ac electric field at 298 K. The concentrations are indicated on the two-dimensional plots in the left column. The indirect dimension slices for paradeuterons are shown in the right column.

angle between the two C−D bond vectors of 61° ± 0.5°, essentially as expected. [Error in the bond angle could result from misalignment of the **E** field vector with the static **B** field. Such a misalignment would not effect the splitting of the paradeuteron within experimental error, but might have the effect of reducing the splittings for the meta- and orthodeuterons noticeably.] The slope with respect to the square of the field is somewhat lower than, but within experimental error of, values given in the review by Van Zijl, Ruessink, Bulthuis, and MacLean,[16] and based on the results by Plantega, Van Zijl, and MacLean[11]

$$\Delta\nu = \frac{3}{2}\frac{e^2qQ}{h}\,6.25 \times 10^{-18}E^2 = 1.80 \times 10^{-12}E^2 \quad (22)$$

Splitting values reported in the earlier work by Hilbers and MacLean,[24] as well as Biemond and MacLean,[12] were even larger and could be fit to the expression $\Delta\nu = 2.60 \times 10^{-12}E^2$. However, those data appear to be clearly lower quality in terms of sensitivity and resolution, so it is probably safe to restrict our comparison to the work in ref 11.

TABLE 2: Experimental and Theoretical Splitting Values (in Hz) for Various Nitrobenzene-d_5 Concentrations[a,b]

nitrobenzene-d_5 concn (M)	para-	medium dielectric constant[c]	solvent[d]	Onsager's model for para-	Scholte's model for para-
1	12.3	5.4	3:2	25.9	14.4
2	15.2	8.7	7:1	29.8	15.3
3	18.1	12.0	4:1	31.9	15.7
4	24.2	15.3	4:3	33.2	16.0
5	27.9	18.6	1:1	34.1	16.1
6	30.8	21.9	1:1	34.7	16.3
7	36.1	25.2	0:1	35.2	16.4
8	39.2	28.5	0:1	35.6	16.4
9	46.1	31.7	0:1	35.9	16.5
10 (pure)	53.4	35.0	0:1	36.1	16.5

[a] Mixtures of mineral oil, *p*-xylene, and nitrobenzene-d_5 in the presence of 60 kV/cm electric fields at 298 K were studied. [b] The splitting measurement error was estimated to be 0.5 Hz. [c] Taken as a linear function of the solute molar concentration. [d] Volume of oil: volume of *p*-xylene.

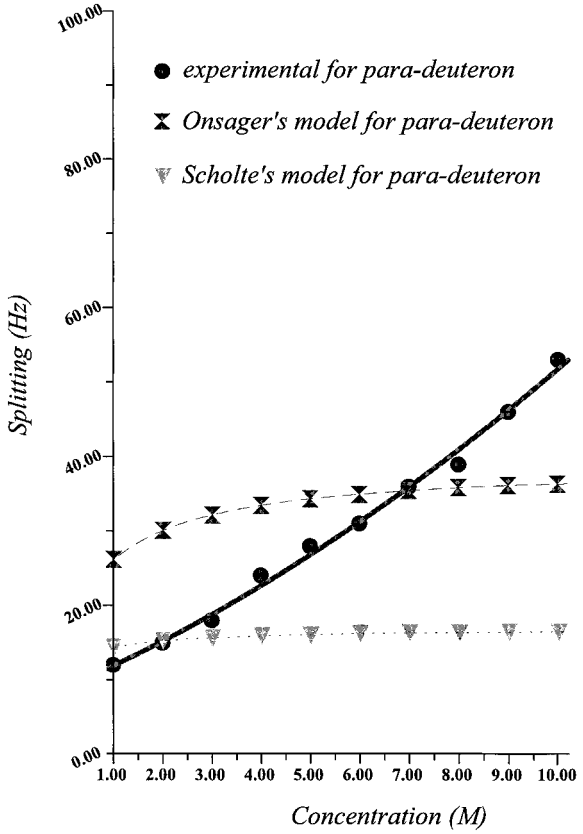

Figure 8. Dependence of the experimental paradeuteron's quadrupolar splittings, as well as the splittings predicted by Onsager's and Scholte's models on the nitrobenzene-d_5 concentration in nonpolar solvents. The exact composition of the solvents is indicated in Table 2. The splittings are much smaller for dilute nitrobenzene than for neat nitrobenzene and agree better with Scholte's than with Onsager's description.

The slope of the field dependence for neat nitrobenzene may not be simple to rationalize and is discussed in the next section. Discussion of the size of the effect will focus on the paradeuteron; due to the geometric effect, this deuteron shows the largest splitting.

Concentration Dependence. For neat nitrobenzene, the theoretically obtained splitting values (vide infra) were uniformly lower than the experimental ones. If nitrobenzene-d_5 was mixed with a nonpolar solvent, much lower splitting values were also

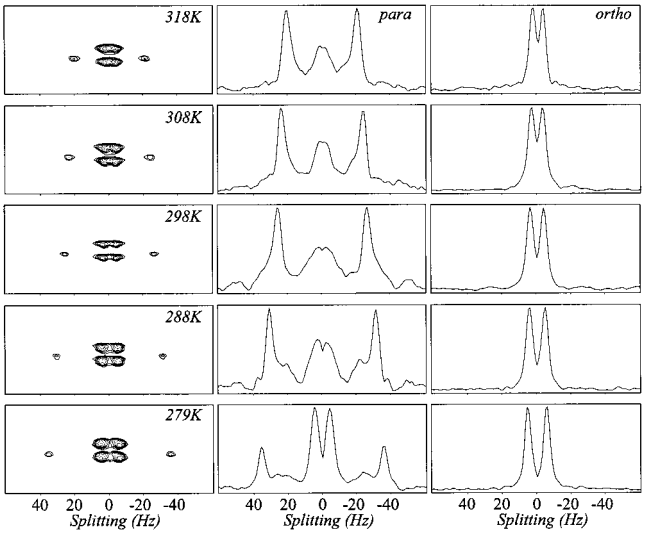

Figure 9. Deuterium spectra of pure nitrobenzene-d_5 at different temperatures in the presence of a 60 kV/cm (rms) external ac electric field. The temperatures are indicated on the two-dimensional plots in the left column. The indirect dimension slices for para- and orthodeuterons are shown in the middle and the right columns. The minor peak in the para spectrum is the meta deuterons.

obtained. The simplest model to account for this effect is a fluctional liquid cluster structure characterized by a preference for head-to-tail arrangements, which leads to an apparent increase in the dipole moment. Onsager's and Scholte's models do not take into account short-range interactions between dipolar nitrobenzene molecules. To compare theoretical and experimental alignment values quantitatively, we conducted more challenging experiments to characterize nitrobenzene alignment at low concentrations in *p*-xylene/mineral oil mixtures which presumably provide a simpler dielectric medium with weaker molecular cluster formation. The 2D and the indirect dimension spectra for paradeuterons of nitrobenzene-d_5 in a mixture of mineral oil and *p*-xylene at various concentrations at 60 kV/cm are shown in Figure 7. The experimental splitting values for each concentration and the corresponding values calculated using Onsager's and Scholte's models are indicated in Table 2 and plotted as a function of concentration in Figure 8. Although the dielectric constant changes by a factor of 5 in the series of solvents, neither Onsager's nor Scholte's models predicts a strong variation in the order parameter. Our data, however, do indicate a strong dependence of the order parameter over the solvent series. Since we assume that short-range interactions and cluster formation are the origin of this variation, we compare the low concentration asymptote of our data to the theoretical models. For practical reasons, the lowest concentration of nitrobenzene was 1 M. Data in Table 2 and Figure 8 indicate that Onsager's model predicts splitting values far higher for the dilute solutions than the experimental values. We found Scholte's model to be in better agreement with our data than Onsager's model, which is not surprising, taking into account the elliptical molecular shape of nitrobenzene. Biemond and MacLean[12] reported a good agreement with Onsager's model predictions for the dilute nitrobenzene-d_5 solutions in benzene. However, as mentioned above, the splitting values measured by these authors at that time were very high in comparison with the later more thorough work.[11] The dependence of the splitting values on concentration, however, agreed well with the present study.

Temperature Dependence. The temperature is also expected to affect the order parameter through Boltzmann averaging in

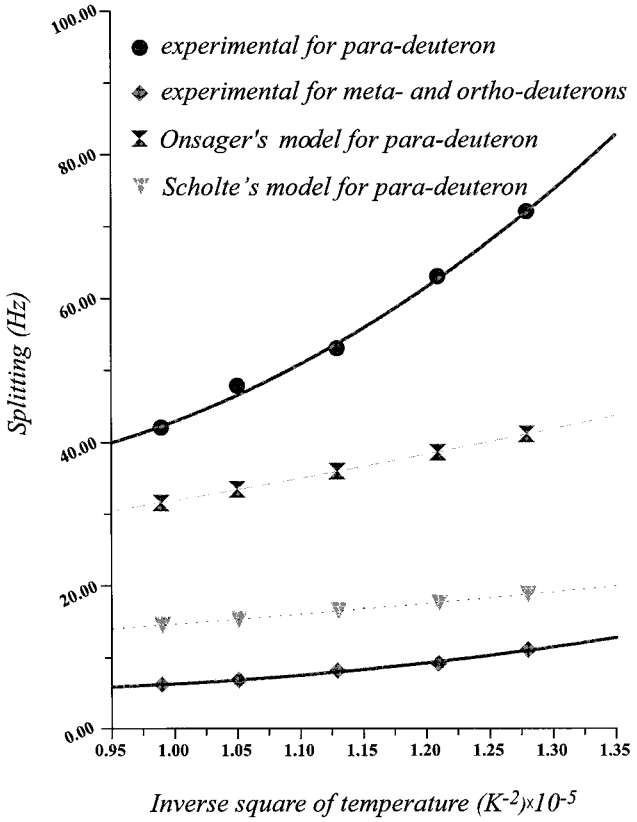

Figure 10. Dependence of the para-, ortho-, and metadeuteron's quadrupolar splitting values, as well as the values obtained from Onsager's and Scholte's models for para-deuteron on the inverse of square of the temperature for pure nitrobenzene-d_5 in the presence of a 60 kV/cm (rms) external ac electric field. The splittings do not follow an inverse square dependence on temperature, presumably because of the changes in the liquid structure over temperature.

the degree of alignment, and indeed had a strong effect on our observed splittings. 2D as well as the indirect dimension spectra for para- and orthodeuterons for pure nitrobenzene-d_5 at 60 kV/cm field are illustrated in Figure 9 for temperatures ranging from 279 to 318 K. Figure 10 shows the experimental splitting values for para-, ortho-, and metadeuterons, as well as the values predicted by Onsager's and Scholte's models for paradeuteron as a function of the inverse of square of the temperature. The data deviate substantially from this expected dependence. Apart from the greater thermal competition with the alignment, the increase in temperature could disrupt short-range molecular interactions. Better agreement with the theoretical splitting values occurs at higher temperatures, and thus we assume that the molecular clusters form more strongly at lower temperatures, as expected if the process is enthalpically driven.

Conclusions

A homogeneous pulsed ac electric field applied to nitrobenzene samples in an electric field cell was used to induce molecular order parameters of order 10^{-4}, which were demonstrated using 2D NMR experiments. Pulsed ac electric fields rather then dc fields offered technical advantages related mainly to avoiding sample degradation. Observed splittings varied with the applied field strength and temperature as expected, and were in reasonable agreement with previous NMR determinations involving dc fields, with molecular geometric considerations, and with electrostatic predictions for dilute solutions. Thus, we validated our measurements in preparation for future investiga-

tions. Real-time control on the degree of molecular alignment holds promise for pulse sequences in which time dependent rf and electrical modulations are synchronized.

Acknowledgment. The authors thank Dr. Lorenz Mitschang for help with the pulse sequence development, as well as Dr. Peter Osman, Dr. Bruce Brunschwig, and Dr. James Lux for advice on sample preparation. This project was supported by the Department of Energy (Grant DE-FG02-95ER14508), Training Program in Molecular Biophysics (2T32 GM08281), and by R. C. Cottrell (CS 0046).

References and Notes

(1) Gayathri, C.; Bothner-By, A. A.; VanZijl, P. C. M.; MacLean, C. *Chem. Phys. Lett.* **1982**, *87*, 192.

(2) Tolman, J. R.; Flanagan, J. M.; Kennedy, M. A.; Prestegard, J. H. *Proc. Natl. Acad. Sci.* U.S.A. **1995**, *92* (20), 9279.

(3) Tjandra, N.; Bax, A. *Science* **1997**, *278*, 1111.

(4) Ottiger, M.; Delaglio, F.; Marquardt, J. L.; Tjandra, N.; Bax, A. *J. Magn. Reson.* **1998**, *134*, 365.

(5) Kushida, T.; Saiki, K. *Phys. Rev. Lett.* **1961**, *7*, 9.

(6) Armstrong, J.; Bloembergen, N.; Gill, D. *Phys. Rev. Lett.* **1961**, *7*, 11.

(7) Gill, D.; Bloembergen, N. *Phys. Rev.* **1962**, *129*, 2398.

(8) Collins, F. A.; Bloembergen, N. *J. Chem. Phys.* **1964**, *40*, 3479.

(9) Hilbers, C. W.; MacLean, C. *NMR Basic Princ. Prog.* **1972**, *7*, 1.

(10) Huis, L.; Decanter, F. J. J.; MacLean, C. *Mol. Phys.* **1991**, *73*, 1077.

(11) Plantenga, T. M.; VanZijl, P. C. M.; MacLean, C. *Chem. Phys.* **1982**, *66*, 1.

(12) Biemond, J.; MacLean, C. *Mol. Phys.* **1973**, *26*, 409.

(13) Osman, P.; Cornell, B. *Biochim. Biophys. Acta* **1994**, *1195*, 197.

(14) Abragam, A. *The Principles of Nuclear Magnetism*; Clarendon Press: Oxford, UK, 1961.

(15) Spiess, H. W. *NMR Basic Princ. Prog.* **1978**, *15*, 55.

(16) VanZijl, P. C. M.; Ruessink, B. H.; Bulthuis, J.; MacLean, C. *Acc. Chem. Res.* **1984**, *17*, 172.

(17) Wei, I. Y.; Fung, B. M. *J. Chem. Phys.* **1970**, *52*, 4917.

(18) Stark, R. E.; Vold, R. L.; Vold, R. R. *Chem. Phys.* **1977**, *20*, 337.

(19) Hill, N. E. *Dielectric properties and molecular behaviour*; The Van Nostrand Series in Physical Chemistry; Sugden, T. M., Ed.; Van Nostrand Reinhold: London, 1969.

(20) Onsager, L. *J. Am. Chem. Soc.* **1936**, *58*, 1486.

(21) Bottcher, C. J. F. *Theory of Electric Polarization*, 2nd ed.; Elsevier: Amsterdam, 1973; Vol. 1.

(22) Scholte, T. G. *Leiden* **1950**.

(23) Osborn, J. A. *Phys. Rev.* **1945**, *67*, 351.

(24) Hilbers, C. W.; MacLean, C. *Mol. Phys.* **1969**, *17*, 433.